Synthesis and Characterization of 4-Methoxy-7-nitroindolinyl-D-aspartate, a Caged Compound for Selective Activation of Glutamate Transporters and *N*-Methyl-D-aspartate Receptors in Brain Tissue†

Yanhua H. Huang,‡ Saurabh R. Sinha,‡ Olesya D. Fedoryak,§ Graham C. R. Ellis-Davies,*,§ and Dwight E. Bergles*,‡

Department of Pharmacology and Physiology, Drexel University College of Medicine, 245 North 15th Street, Philadelphia, Pennsylvania 19102, and Department of Neuroscience, Johns Hopkins University Medical School, 725 North Wolfe Street, WBSB 813, Baltimore, Maryland 21205

Received September 9, 2004; Revised Manuscript Received November 16, 2004

ABSTRACT: The D-isomer of aspartate is efficiently transported by high-affinity Na^+/K^+-dependent glutamate transporters and is an effective ligand of *N*-methyl-D-aspartate (NMDA) receptors. To facilitate analysis of the regulation of these proteins in their native membranes, we synthesized a photolabile analogue of D-aspartate, 4-methoxy-7-nitroindolinyl-D-aspartate (MNI-D-aspartate). This compound was photolyzed with a quantum efficiency of 0.09 at pH 7.4. Photorelease of D-aspartate in acute hippocampal slices through brief (1 ms) UV laser illumination of MNI-D-aspartate triggered rapidly activating currents in astrocytes that were inhibited by the glutamate transporter antagonist DL-threo-β-benzyloxyaspartic acid (TBOA), indicating that they resulted from electrogenic uptake of D-aspartate. These transporter currents exhibited a distinct tail component that was ~2% of the peak current, which may result from the release of K^+ into the extracellular space during counter transport. MNI-D-aspartate was neither an agonist nor an antagonist of glutamate transporters at concentrations up to 500 μM and was stable in aqueous solution for several days. Glutamate transporter currents were also elicited in Bergmann glial cells and Purkinje neurons of the cerebellum in response to photolysis of MNI-D-aspartate, indicating that this compound can be used for monitoring the occupancy and regulation of glutamate transporters in different brain regions. Photorelease of D-aspartate did not activate α-amino-3-hydroxy-5-methyl-4-isoxazolepropionic acid (AMPA)/kainate receptors or metabotropic glutamate receptors (mGluRs) in neurons, but resulted in the selective, but transient, activation of NMDA receptors in hippocampal pyramidal neurons; MNI-D-aspartate was not an antagonist of NMDA receptors. These results indicate that MNI-D-aspartate also may be useful for studying the regulation of NMDA receptors at excitatory synapses.

Glutamate released at synapses during excitatory neurotransmission in the mammalian central nervous system is ultimately removed from the extracellular space by high-affinity Na^+- and K^+-dependent glutamate transporters. By preventing glutamate accumulation, these transporters help to preserve the fidelity of transmission and prevent excitotoxicity (*1*, *2*). In addition to these homeostatic functions, glutamate transporters act on a rapid time scale to shape the activation of receptors, particularly NMDA (*N*-methyl-D-aspartate)[1] receptors and mGluRs in extrasynaptic domains (*3*−*8*), and to limit spillover of glutamate between neighboring synapses (*9*, *10*). These results suggest that acute or prolonged changes in the expression or activity of glutamate transporters could significantly alter signaling at excitatory synapses, network activity, and the extent of excitotoxic damage after injury or disease. However, the mechanisms responsible for regulating glutamate transporter activity in situ are not well understood.

Glutamate transporter activity can be monitored through uptake of radiolabeled substrates, through optical measurements of cytosolic pH changes or absorbance of voltage-sensitive dyes, or by recording transporter-associated charge movements (*11*). Glutamate uptake leads to net charge movement, because two positive charges are carried into the cell during each cycle of transport (*12*, *13*), and binding of

† Supported by the Human Frontier Science Program Organization (GED), the NIH (GM65473 and GM53395 to GED; NINDS 44564 to DEB), the NSF (BD0090826 to GED), the McKnight Endowment Fund for Neuroscience (GED), and the Robert Packard Center for ALS Research at Johns Hopkins (DEB). D.E.B. is an Alfred P. Sloan Research Fellow.

* To whom correspondence should be addressed. G.C.R.E.-D.: telephone, (215) 762-8794; fax, (215) 762 2299; e-mail, ged@drexel.edu. D.E.B.: telephone, (401) 955-6939; fax, (410) 955-6942; e-mail, dbergles@jhmi.edu.

‡ Johns Hopkins University Medical School.

§ Drexel University College of Medicine.

[1] Abbreviations: NMDA, *N*-methyl-D-aspartate; AMPA, α-amino-3-hydroxy-5-methyl-4-isoxazole propionic acid; TBOA, DL-threo-β-benzyloxyaspartic acid; MNI-D-aspartate, 4-methoxy-7-nitroindolinyl-D-aspartate; mGluRs, metabotropic glutamate receptors; MNI-L-glutamate, 4-methoxy-7-nitroindolinylglutamate; CNB, α-carboxynitrobenzyl; EAAC1, excitatory amino acid carrier 1; ACSF, artificial cerebral spinal fluid; GABA, γ-aminobutyric acid; GLAST, glutamate-aspartate transporter; EAAT, excitatory amino acid transporter; GLT-1, glutamate transporter 1; LY 367385, (*S*)-(+)-α-Amino-4-carboxy-2-methylbenzeneacetic acid; TEA, tetroethylammonium; THA, D,L-*threo*-3-hydroxyaspartate.

10.1021/bi048051m CCC: $30.25
Published on Web 02/12/2005

glutamate to the transporter increases its conductance to certain anions (*14*). Transporter-associated currents are proportional to the movement of glutamate (*12*, *15*), providing a means to monitor glutamate transporter activity in individual cells with high temporal fidelity. Glutamate transporter currents can be elicited from astrocytes in brain slices following stimulation of excitatory afferents (*16*), by bath application of substrate, by focal application of substrate using pressure, or by photolysis of caged substrates (*6*). The analysis of synaptic transporter currents is complicated by the dependence on nerve terminals for glutamate, while bath application is very slow and lacks spatial precision. Pressure application improves temporal and spatial resolution but requires positioning of the application pipet within tissue, and responses elicited using this approach exhibit poor stability due to repeated mechanical disruption of surrounding tissue. In contrast, photolysis of caged substrates allows rapid and focal activation of transporters, in a manner free from mechanical artifact.

An ideal caged compound should have the following properties: (1) it must be biologically inert (neither an agonist or antagonist), (2) the compound should be rapidly released upon photolysis (release half-time < 20 μs), (3) uncaging should make efficient use of the incident light (exhibit a large extinction coefficient and quantum yield), (4) the caging group byproduct should not exhibit activity nor be harmful to cells, and (5) the caged compound must not undergo spontaneous hydrolysis during storage or in physiological buffer. For studies of high-affinity receptors such as transporters (K_m range 4−97 μM) (*17*) and NMDA receptors (K_m ~ 5 μM) (*18*), this latter property is particularly important, as this free substrate will alter baseline conditions by causing activation in the absence of light. Our previous studies indicate that MNI-caged L-glutamate (MNI-L-glutamate) is very stable (*24*), and this knowledge was a prime driving force for the synthesis of MNI-D-aspartate. Although L-glutamate is the primary physiological substrate of glutamate transporters, caged versions of L-glutamate are of limited use for studying the interaction of glutamate receptors and glutamate transporters in situ, as the liberated L-glutamate will act on receptors and transporters simultaneously (*19*). In contrast, D-aspartate offers significant advantages, as it is efficiently transported (*17*) but it is unlikely to have appreciable activity at AMPA receptors, kainate receptors, or mGluRs. A previous report described the synthesis of an CNB-caged D-aspartate and showed that this compound could be used to study the activation kinetics of EAAC1, the primary neuronal glutamate transporter, when heterologously expressed in HEK293 cells (*20*). However, this caged compound has been reported to be somewhat unstable, a common problem of excitatory amino acids caged with CNB (*21*), and its activity at glutamate transporters in situ has not been examined.

Here we describe the synthesis of a novel caged form of D-aspartate (MNI-D-aspartate), in which the β-carboxylate of D-aspartate is coupled to 4-methoxy-7-nitroindolinyl (MNI) through a photolabile amidic bond (*22*), and examine the responses triggered in neurons and glial cells in acute brain slices upon photolysis. MNI-D-aspartate is stable in solution, can be photolyzed rapidly, and is biologically inert. Upon brief exposure to near-UV light, this compound reliably evoked glutamate transporter currents in astrocytes, Bergmann glial cells, and Purkinje cells, as well as NMDA receptor currents in pyramidal neurons; however, it did not evoke AMPA/kainate or metabotropic glutamate receptor currents. Thus, MNI-D-aspartate can be used to activate glutamate transporters and NMDA receptors in native membranes and to reveal the interactions between receptors and transporters at excitatory synapses in acute brain slices.

MATERIALS AND METHODS

Synthesis of MNI-D-aspartate

General Remarks. Silica gel 60 (mesh 63−200 micron) was used for flash chromatography. A Beckman System Gold fitted with Hamilton PRP-1 columns (4.1 × 250 mm, or 20.1 × 250 mm) was used for HPLC. ^{1}H and ^{13}C NMR were measured on a Varian Mercury 300.

Synthesis. (1) N-(tert-Butoxycarbonyl)-D-aspartic acid α-tert-butyl ester (**2**) was prepared according to a published procedure (*23*).

*(2) 4-Methoxyindolinyl N-(tert-Butoxycarbonyl)-D-aspartic Acid α-tert-Butyl Ester (**3**).* *N*-(*tert*-Butoxycarbonyl)-D-aspartic acid α-*tert*-butyl ester (356 mg, 1.23 mmol), 1,3-dicyclohexylcarbodiimide (254 mg, 1.23 mmol), and 4-(dimethylamino)pyridine (150 mg, 1.23 mmol) were added to a solution of 4-methoxyindoline (142 mg, 0.95 mmol), synthesized as described previously (*24*), in dichloromethane (7 mL). The reaction mixture was stirred at room temperature for 20 h and then it was filtered, diluted with CH_2Cl_2, and washed with saturated $NaHCO_3$ solution, 0.5 N HCl, and brine. The organic layer was dried ($MgSO_4$) and evaporated to dryness. The crude product was purified by flash column chromatography (ethyl acetate/hexane 1:3) to yield product **3** as white solid (357 mg, 0.85 mmol, 89%): ^{1}H NMR ($CDCl_3$) δ 7.8 (1H, d, $J = 8.1$ Hz), 7.15 (1H, t, $J = 8.1$ Hz), 6.58 (1H, d, $J = 8.1$ Hz), 5.82 (1H, d, $J = 8.9$ Hz), 4.48 (1H, m), 4.04 (2H, t, $J = 8.2$ Hz), 3.83 (3H, s), 3.1 (3H, m), 2.83 (1H, dd, $J = 4.0$, 16.8 Hz), 1.45 (9H, s), 1.44 (9H, s); ^{13}C NMR ($CDCl_3$) δ 170.6, 168.6, 156.0, 155.9, 144.1, 129.1, 118.5, 110.2, 106.4, 82.1, 79.8, 55.6, 50.9, 48.7, 38.7, 28.7, 28.3, 25.5; IR (neat) 3440, 3040, 2980, 2938, 1740, 1710, 1660, 1610, 1490, 1465, 1415, 1365, 1340, 1150, 1060, 840 cm^{-1}; MS (ESI) *m*/*z* 421.2 ($M + H^+$).

*(3) 4-Methoxy-7-nitroindolinyl N-(tert-Butoxycarbonyl)-D-tert-butylaspartic Acid (**4**).* To a solution of **3** (357 mg, 0.85 mmol) and silver nitrate (0.287 g, 1.7 mmol) in acetonitrile (10 mL) was added a solution of acetyl chloride (0.133 g, 1.7 mmol) in acetonitrile (5 mL). The reaction mixture was filtered; the filtrate was diluted with ethyl acetate and washed with saturated solution of sodium bicarbonate. The solvent was removed by rotary evaporation, leaving a dark orange oil, which was purified over silica gel using ethyl acetate/hexane (1:2) to yield 251 mg (0.54 mmol, 64%) of product **5**: ^{1}H NMR ($CDCl_3$) δ 7.74 (1H, d, $J = 9.0$ Hz), 6.63 (1H, d, $J = 9.0$ Hz), 5.67 (1H, broad d, $J = 8.1$ Hz), 4.44 (1H, m), 4.22 (2H, t, $J = 8.1$ Hz), 3.90 (3H, s), 3.16 (1H, dd, $J = 4.1$, 16.5 Hz), 3.07 (2H, t, $J = 8.1$ Hz), 2.97 (1H, dd, $J = 4.1$, 16.5 Hz), 1.47 (9H, s), 1.42 (9H, s); ^{13}C NMR ($CDCl_3$) δ 170.0, 169.1, 158.8, 155.8, 136.4, 135.4, 125.5, 122.8, 106.5, 82.4, 79.8, 56.1, 51.1, 49.0, 37.7, 28.6, 28.1, 26.5; IR (neat) 3420, 3050, 2980, 2930, 1740, 1710, 1680, 1610, 1590, 1530, 1490, 1450, 1390, 1365, 1340, 1270,

1250, 1230, 1150, 1080, 1050, 890, 750, 700 cm^{-1}; MS (ESI) *m*/*z* 488.2 ($M + Na^+$).

*(4) 4-Methoxy-7-nitroindolinyl-*D*-aspartic Acid (**1**).* TFA (0.7 mL) was slowly added to a solution of compound **4** (113 mg, 0.24 mmol) in dichloromethane (3 mL). The reaction mixture was stirred at room temperature for 20 h and then the solvent was removed and the crude material was purified by preparative HPLC (isocratic elution with 20% CH_3CN in H_2O) to yield 37 mg (0.12 mmol, 50%) of product **1**: ^1H NMR (D_2O) δ 7.78 (1H, d, $J = 9.3$ Hz), 6.88 (1H, d, $J = 9.3$ Hz), 4.43 (1H, t, $J = 5.0$ Hz), 4.29 (2H, t, $J = 8.0$ Hz), 3.94 (3H, s), 3.39 (2H, m), 3.08 (2H, t, $J = 8.0$ Hz); ^{13}C NMR (D_2O) δ 171.0, 169.2, 159.5, 135.0, 134.3, 125.7, 123.9, 108.3, 56.3, 50.5, 49.7, 34.9, 26.1; MS *m*/*z* 307.8 ($M - H^+$).

Quantum Yield. The quantum yield for uncaging MNI-D-aspartate was measured by comparing the time of photolysis with the filtered (280−400 nm) output of a 500 W medium-pressure Hg lamp of an equimolar solution (250 μM) of MNI-L-glutamate and MNI-D-aspartate in HEPES ACSF. Inosine was used as an inert internal standard (*25*). The path length of the cuvette was 0.1 mm.

Slice Preparation and Electrophysiology

Slice Preparation. Hippocampal slices were prepared from 12−17-day-old Sprague−Dawley rats in accordance with a protocol approved by the Animal Care and Use Committee at Johns Hopkins University. Rats were deeply anesthetized with halothane and decapitated, the hippocampi were dissected free, mounted in agar blocks, cut in 400 μm thick transverse sections using a vibratome (VT1000S, Leica), in oxygenated ice-cold artificial cerebrospinal fluid (ACSF) containing (in mM) NaCl (119), KCl (2.5), $CaCl_2$ (2.5), $MgCl_2$ (1.3), NaH_2PO_4 (1), $NaHCO_3$ (26.2), and D-glucose (11). Slices were allowed to recover on a gauze net submerged in ACSF at 37 °C for 30 min and kept at room temperature thereafter. For cerebellar slices, 250 μm thick parasagittal sections were prepared. Brain slices were used within 7 h of preparation.

Whole Cell Recording. Brain slices that had recovered for at least 1 h were transferred to a Lucite chamber with a coverslip bottom and continuously superfused with oxygenated ACSF. Individual cells (astrocytes, CA1 pyramidal neurons, Bergmann glial cells, or Purkinje neurons) were visualized through a 40× water immersion objective (Olympus LUMPlanFl, NA = 0.8) using an upright microscope (Axioskop FS2, Zeiss) equipped with infrared-Nomarski optics and a CCD camera (Sony XC-73). Recording electrodes were pulled from glass capillary tubing and had a combined resistance of 1.5−3.0 MΩ when filled with the internal solution. For astrocytes and Bergmann glial cells, the internal solution contained (in mM) KCH_3O_3S (KMeS) (120), EGTA (10), HEPES (20), $MgCl_2$ (1), Na_2ATP (2), and NaGTP (0.2); the pH was 7.3. For neuronal recordings the internal solution contained (in mM) $CsCH_3O_3S$ (CsMeS) (105), TEA-Cl (20), EGTA (10), HEPES (20), $MgCl_2$ (1), QX-314 (1), Na_2ATP (2), and NaGTP (0.2); the pH was 7.3. To record transporter-associated anion currents from Purkinje neurons, the internal solution contained (in mM) $CsNO_3$ (100), TEA-Cl (20), EGTA (10), HEPES (20), $MgCl_2$ (1), QX-314 (1), Na_2ATP (2), and NaGTP (0.2); the pH was 7.3. With these solutions the series resistance during recordings was <10 MΩ and was left uncompensated. Unless stated otherwise, holding potentials have not been corrected for the junction potential. Whole-cell currents were amplified using an Axopatch 200B (Axon Instruments), filtered at 2−5 kHz and sampled at 10−20 kHz. A 0.5−5 mV step was applied at the beginning of each trace to measure both the membrane and access resistances. Perforated patch recordings were performed in the cell attached patch mode by including Amphotericin-B (120 μg/mL) in the KMeS internal solution.

Solution Application. Caged compounds were dissolved in HEPES-buffered saline (HEPES ACSF) containing (in mM) NaCl (137), KCl (2.5), $CaCl_2$ (2.5), $MgCl_2$ (1.3), and HEPES (20); the pH was 7.3. Solutions containing caged compounds were applied to the slice using a wide-bore (tip diameter 50−100 μm) pipet connected to a manifold fed by four 10 mL reservoirs. Solutions were switched by alternately opening and closing valves attached to each reservoir. Antagonists were used to block voltage-gated Na^+ channels (tetrodotoxin, TTX; 1 μM), AMPA/kainate receptors (2,3-dioxo-6-nitro-1,2,3,4-tetrahydrobenzo[*f*]quinoxaline-7-sulfonamide disodium salt, NBQX; 10 μM), NMDA receptors [(*RS*)-3-(2-carboxypiperazin-4-yl)propyl-1-phosphonic acid, *R*,*S*-CPP (10 μM); (5*R*,10*S*)-(+)-5-methyl-10,11-dihydro-5*H*-dibenzo[*a*,*d*]cyclohepten-5,10-imine hydrogen maleate, MK-801 (50 μM)], and $GABA_A$ receptors (6-imino-3-(4-methoxyphenyl)-1(6*H*)-pyridazinebutanoic acid dihydrobromide, SR-95531; 5 μM). In some experiments, group I mGluRs were blocked with LY367385 (100 μM). Glutamate transporters were inhibited using DL-threo-β-benzyloxyaspartic acid (TBOA, 100−200 μM). The specific blockers used in each experiment are indicated in the figure legends. For each experiment, the caged compound solution contained the same concentration of antagonists present in the bath solution. In some experiments, D-aspartate (500 μM dissolved in HEPES ACSF) was applied locally through a small-tip pipet (~1 μm diameter) using a picospritzer (Pressure System IIe, Toohey Co.); a 5−10 ms pulse of 15−20 psi was used to eject the solution. All appropriate blockers were included in the puffer pipet solution.

Photolysis of Caged Compounds. For photolysis, an argon ion laser (Stabilite 2017-AR, Spectra-Physics) providing ~230 mW or 380 mW of multi-line UV light (333.6−363.8 nm) was coupled to the microscope through a multimode quartz fiber optic cable (Oz Optics Ltd.). The output of the fiber optic was collimated using a quartz lens, projected through the fluorescence port of a Zeiss Axioskop FS2 microscope, and focused to a ~50 μm spot using a 40× water immersion objective (Olympus LUMPlanFl) or to a ~100 μm spot using a 20× water immersion objective (Olympus UMPlanFl). The UV spot was centered on the soma of astrocytes or pyramidal cells or on the dendritic arbor of the Purkinje cells, using a targeting laser (633 nm HeNe). To control the length of exposure, a computer-controlled, programmable pulse generator (Master 8, AMP Instruments) was used to trigger a high-speed laser shutter (NM laser) placed between the laser head and the fiber launch. Photolysis was achieved by opening the shutter for 1 ms. In some experiments, the intensity of the laser was varied using the aperture on the laser head. The output intensity for each aperture was measured using a power meter. A laser intensity (at the output) of 230 mW was used

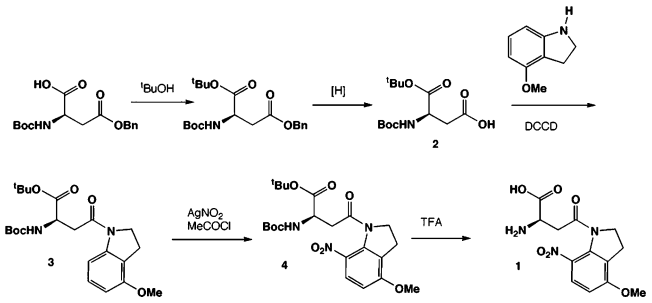

FIGURE 1: Synthesis and structure of MNI-D-aspartate.

for recordings from astrocytes, Bergmann glial cells, and pyramidal neurons (40× objective), corresponding to a total light energy of 29 mJ/cm^2. An intensity of 380 mW was used for recordings from Purkinje neurons (20× objective), corresponding to a total light energy of 48 mJ/cm^2. These values reflect the laser power prior to entering the fiber optic; the energy reaching the cell is likely to be considerably less due to loss at the fiber launch, the microscope lenses, and the intervening tissue.

Chemicals Used for Photolysis Experiments. MNI-L-glutamate, NBQX, *R,S*-CPP, MK-801, LY367385, SR-95531, and TBOA were purchased from Tocris. D-Aspartate was purchased from Sigma. TTX and QX-314 (*N*-(2,6-dimethylphenylcarbamoylmethyl)triethylammonium chloride) were purchased from Alomone Labs.

Data Analysis and Statistics. Data were analyzed off-line using Clampfit (Axon Instruments) and Origin (Microcal) software. For experiments on astrocytes, only cells in which the amplitude of the response to a −5 mV step changed by less than 25% during the course of an experiment were analyzed. All values are represented as mean ± standard error of the mean. The Student's *t*-test (paired or unpaired, as appropriate) was used for statistical comparison; $p < 0.05$ was considered significant. The rise time of responses was calculated from 10−90% of the peak response, and the τ decay was measured using a single-exponential least-squares fit. Half-decay refers to the time required for the response to decay to 50% of the peak amplitude.

RESULTS

Synthesis and Quantum Yield of MNI-D-aspartate. The steps involved in the synthesis of MNI-D-aspartate are outlined in Figure 1. The requisitely protected D-aspartate was synthesized in the same manner as reported previously for L-aspartate (*23*) in a yield of 73%. The β-carboxylate was coupled to 4-methoxyindoline (*24*) using standard DCCD/DMAP conditions to give **3** in a yield of 89%. The essential nitro functionality was introduced into intermediate **3** using silver nitrate and acetyl chloride (*26*) to give 7-nitroindoline **4**, along with the undesired 5-nitro isomer. The yield of **4** after flash chromatography was 64% (the 7- and 5-nitro isomers could easily be separated at this stage, unlike MNI-L-glutamate). The BOC and *tert*-butyl protecting groups were removed by treatment of **4** with TFA to give the target caged D-aspartate, **1**, in a yield of 50% after HPLC purification. HPLC purification of MNI-D-aspartate was essential to remove free D-aspartate.

Quantum Yield of Photolysis. The quantum yield of uncaging of MNI-D-aspartate was determined by direct comparison with MNI-L-glutamate. Both caged compounds

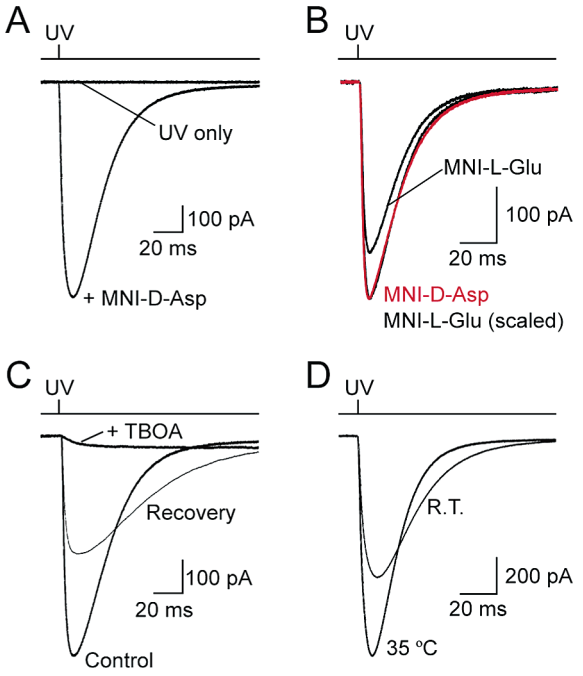

FIGURE 2: Photolysis of MNI-D-aspartate activates glutamate transporter currents in hippocampal astrocytes. (A) A transient inward current was elicited in an astrocyte by a 1 ms flash of UV laser light in the presence but not in the absence of MNI-D-aspartate (MNI-D-Asp, 125 μM). The trace above shows the duration of UV exposure. (B) The response elicited by photolysis of MNI-D-aspartate (MNI-D-Asp, 125 μM, red trace) exhibited similar kinetics to the response elicited by photolysis of MNI-L-glutamate (MNI-L-Glu, 125 μM). (C) The current evoked by photolysis of MNI-D-aspartate was reversibly inhibited by TBOA (200 μM). (D) The glutamate transporter current evoked in astrocytes by photolysis of MNI-D-aspartate exhibited a larger peak amplitude and faster decay at near physiological temperature. (R.T., room temperature). All recordings were made from astrocytes located in stratum radiatum of area CA1, in the presence of TTX (1 μM), *R,S*-CPP (10 μM), MK-801 (50 μM), and NBQX (10 μM). Astrocytes were voltage-clamped at −80 mV with a KMeS-based internal solution.

have the same extinction coefficient, so analysis of the irradiation of an equimolar solution of both compounds, to test the relative extent of photolysis, yields the quantum of MNI-D-aspartate uncaging. We found that when a solution containing 0.25 mM of each compound was irradiated (total OD = 0.215, to ensure uniform photolysis), the quantum yield was 0.09 ± 0.01 ($n = 3$), slightly faster than that of MNI-L-glutamate (*24*).

Photolysis of MNI-D-aspartate Triggers Glutamate Transporter Currents in Astrocytes. Glutamate transporters are present at a high density in the membranes of astrocytes in the hippocampus (*27*), and application of L-glutamate through pressure or photolysis in brain slices induces an inward current in astrocytes that is blocked by glutamate transporter antagonists (*6*, *16*). To determine whether photolysis of MNI-D-aspartate is also capable of eliciting glutamate transporter currents in situ, we made whole-cell voltage-clamp recordings from astrocytes in the CA1 region of hippocampus and measured their response to UV light in the presence of MNI-D-aspartate. When the ACSF contained antagonists of AMPA, NMDA, and $GABA_A$ receptors, as well as TTX (see Materials and Methods) to block possible indirect effects resulting from excitation of surrounding neurons, brief (1 ms) exposure to laser UV light produced a rapidly activating, transient, inward current in astrocytes (Figure 2A) that was

only observed when the superfusing solution contained MNI-D-aspartate (125 μM). These currents had a slightly faster rise time than responses elicited by photolysis of 125 μM MNI-L-glutamate (rise time: MNI-D-aspartate, 3.1 $\pm$ 0.2 ms; MNI-L-glutamate, 3.5 $\pm$ 0.2 ms, $p < 0.001$) but slightly slower decay kinetics (decay τ: MNI-D-aspartate, 16.9 $\pm$ 0.9 ms, $n = 11$; MNI-L-glutamate, 15.4 $\pm$ 0.6 ms, $p < 0.05$, $n = 11$) (Figure 2B) (*6*). The peak amplitude of these responses was reduced by 94.5 $\pm$ 0.6% ($n = 4$) by TBOA (200 μM), a selective antagonist of glutamate transporters (*28*, *29*) (Figure 2C). These currents reflect the movement of charges that are directly coupled to the flux of glutamate, as they were recorded with an internal solution (KMeS) that does not reveal the glutamate transporter-associated anion conductance (*30*). Increasing the temperature from room temperature (22−24 °C) to near physiological temperature (34−36 °C) increased the amplitude of these responses by 34.1 $\pm$ 6.2% ($p < 0.01$) and decreased the rise time by 10.0 $\pm$ 3.5% ($p < 0.05$) and the decay time by 29.9 $\pm$ 2.6 % ($n = 5$, $p < 0.001$) (Figure 2D), in accordance with the high temperature dependence exhibited by glutamate transporters (*31*, *32*). However, the charge transfer induced by these currents was similar at higher temperature (5.0 $\pm$ 3.2% increase, $p = 0.099$, $n = 5$), suggesting that a comparable amount of D-aspartate was transported at both temperatures. These results indicate that laser-induced photolysis of MNI-D-aspartate releases the free amino acid, which is then removed by glutamate transporters in astrocyte membranes.

By varying the intensity of UV light, it was possible to control the amount of D-aspartate liberated. As shown in Figure 3A, the peak amplitude of astrocyte transporter currents increased monotonically with increasing laser power, suggesting that glutamate transporters were operating in a linear range of their dose-response curve under these conditions. As expected from the concentration dependence of binding, the rise times of glutamate transporter currents became faster as the laser intensity was increased, from 2.1 $\pm$ 0.1 ms at 50% laser power to 1.7 $\pm$ 0.1 ms ($n = 3$, $p < 0.01$) at 100% (relative) power (230 mW at laser output; 50 μm spot illumination), similar to concentration-dependent effects on transporter currents observed in outside-out patches removed from astrocytes (*16*). However, unlike responses recorded from patches, photolysis-induced glutamate transporter currents recorded in situ became more prolonged as more D-aspartate was released (half-decay time: 50% relative intensity, 22.8 $\pm$ 4.1 ms; 100% relative intensity, 27.2 $\pm$ 4.5 ms, $n = 3$, $p < 0.01$), suggesting that clearance from within the tissue is delayed as more D-aspartate is liberated or that additional GLAST transporters, which exhibit a lower affinity and slower transport rate for D-aspartate (*17*), are recruited at higher laser intensities.

In addition to the transient response, glutamate transporter currents recorded from astrocytes exhibited a slowly decaying "tail current" that required several seconds to return to baseline (Figure 3B), similar to transporter currents evoked in astrocytes through synaptic release (*16*). The amplitude of this prolonged inward current was ~2% of the peak, and this proportion remained fixed at all laser intensities (Figure 3B). This tail current is unlikely to have resulted from activation of voltage-gated channels in surrounding neurons, as UV illumination under these conditions did not elicit a response from surrounding neurons (see Figure 7). These

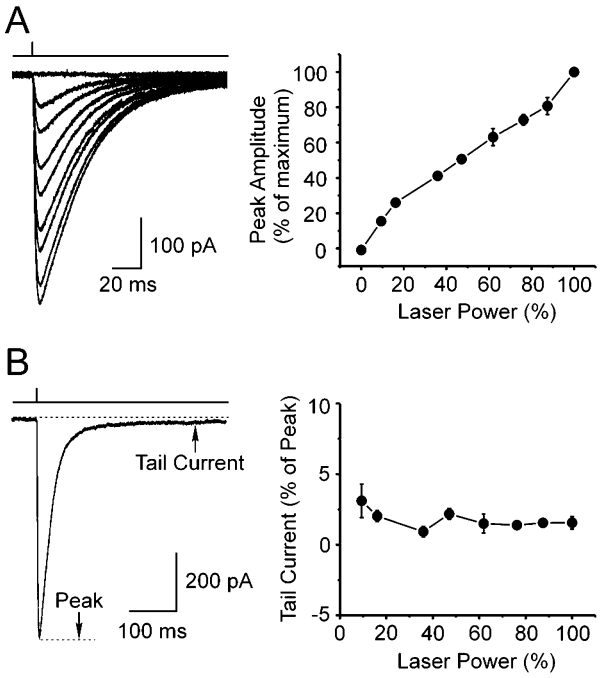

FIGURE 3: Photolysis evoked glutamate transporter currents recorded at different UV light intensities. (A) (Left) Glutamate transporter currents induced in a hippocampal astrocyte by uncaging MNI-D-aspartate (125 μM) with a range of UV light intensities. (Right) Grouped data showing the relationship between light intensity and the normalized peak amplitude of the evoked transporter current ($n = 3$). (B) (Left) A single response recorded from an astrocyte in response to MNI-D-aspartate photolysis illustrating the discrete peak and tail currents. (Right) Grouped data showing the relative amplitude of the tail current (% of peak) at different UV light intensities. The tail current was measured by averaging the current 500−600 ms after the flash ($n = 3$). All recordings were made from astrocytes located in the stratum radiatum of area CA1, in the presence of TTX (1 μM), *R*,*S*-CPP (10 μM), MK-801 (50 μM), and NBQX (10 μM). Astrocytes were voltage-clamped at −80 mV with a KMeS-based internal solution.

results suggest that the photolysis-induced tail current occurs as a direct result of glutamate transporter activation.

Physiological Properties and Aqueous Stability of MNI-D-aspartate. An ideal caged substrate of glutamate transporters should not act as a substrate or an antagonist and should be stable in aqueous solution. To determine whether our new caged compound is a substrate for glutamate transporters, we measured the response of astrocytes to a high concentration of MNI-D-aspartate. Although perfusion of free D-aspartate (500 μM) induced an inward current of −134.7 $\pm$ 41.0 pA ($n = 4$), application of 500 μM MNI-D-aspartate did not elicit a consistent response (−15.2 $\pm$ 11.3 pA, $n = 6$, $p > 0.05$), indicating that the caged compound is not a substrate for glutamate transporters. Although MNI-D-aspartate did not activate glutamate transporters, it could act as an antagonist, similar to the aspartate analogues TBOA and THA (*29*). This is a significant concern because other caged neurotransmitters (e.g., 4-methoxycarbonyl-7-nitroindolinyl-caged-GABA and -glycine) have been demonstrated to have antagonistic properties at their respective receptors (*19*). To determine whether MNI-D-aspartate is an antagonist of glutamate transporters, we examined the effect of the caged compound on responses evoked through local pressure application of D-aspartate (500 μM). As shown in Figure 4A, application of MNI-D-aspartate (500 μM) did not

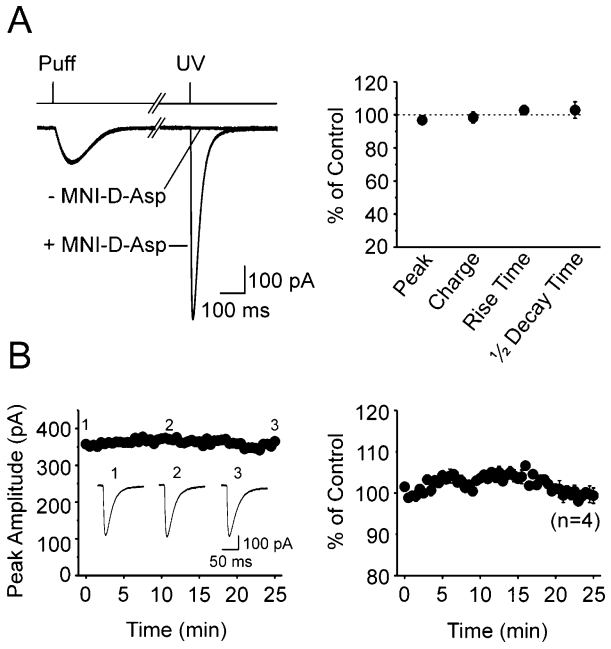

FIGURE 4: MNI-D-aspartate does not antagonize glutamate transporters. (A) (Left) Glutamate transporter currents evoked in a hippocampal astrocyte by local pressure application of D-aspartate (500 μM; pressure pulse, 5−10 ms at 15−20 psi), in the absence and presence of MNI-D-aspartate (MNI-D-Asp, 500 μM). A 1 ms UV flash was applied at the end of the recording to demonstrate the presence of the caged compound. (Right) Grouped data showing the change in peak amplitude, charge transfer, 10−90% rise time, and half-decay time of transporter currents elicited through pressure application of D-aspartate recorded in the absence and presence of MNI-D-aspartate ($n = 4$). (B) (Left) Peak amplitude of glutamate transporter currents recorded from an astrocyte over a period of 25 min in a perforated-patch recording configuration ([MNI-D-aspartate] = 125 μM). Three representative traces are shown in the inset to illustrate the time course of the transporter currents over the duration of the recording. (Right) Grouped data showing normalized peak amplitudes over the 25 min recording period for four experiments. All recordings were made from astrocytes located in stratum radiatum of area CA1, in the presence of TTX (1 μM), *R,S*-CPP (10 μM), MK-801 (50 μM), and NBQX (10 μM). Astrocytes were voltage-clamped at −80 mV with a KMeS-based internal solution.

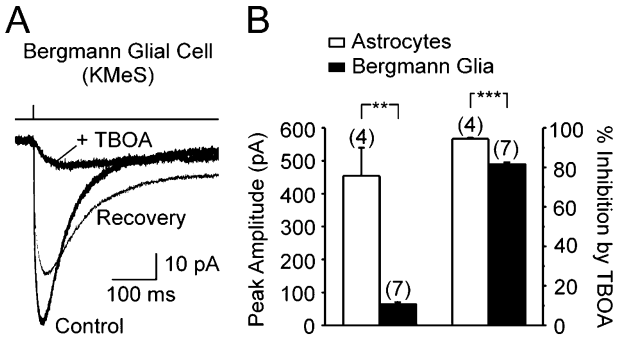

FIGURE 5: Photolysis of MNI-D-aspartate elicits glutamate transporter currents in Bergmann glia of the cerebellum. (A) Inward currents recorded from a Bergmann glial cell in response to photolysis of MNI-D-aspartate (125 μM) were inhibited by the glutamate transporter antagonist TBOA (200 μM). SR-95531 (5 μM), *R,S*-CPP (10 μM), and NBQX (10 μM) were present throughout the experiment. (B) Grouped data comparing the peak amplitudes and percent inhibition by TBOA of responses recorded in Bergmann glia and hippocampal astrocytes in response to photolysis of MNI-D-aspartate. Numbers in parentheses indicate the number of experiments. Transporter currents in each case were recorded with a 40× objective using 125 μM MNI-D-aspartate. Astrocytes and Bergmann glia were voltage-clamped at −80 mV with a KMeS-based internal solution. $^{**}p < 0.01$; $^{***}p < 0.001$.

significantly change the amplitude, charge transfer, or time course of transporter currents induced by D-aspartate, indicating that the caged compound is not a glutamate transporter antagonist. To assess the stability of the caged compound, a 500 μM solution of MNI-D-aspartate was prepared in HEPES-ACSF (pH 7.3), stored at 4 °C in the dark, and applied to astrocytes 2 and 4 days later. This solution produced a change in holding current of 10.0 ± 18.8 pA ($n = 6$) at 2 days and −8.7 ± 3.3 pA ($n = 3$) at 4 days, indicating that this compound is highly stable in aqueous solution. The amplitude of glutamate transporter currents induced by photolysis of MNI-D-aspartate was dependent on the concentration of MNI-D-aspartate, the relative locations of the superfusion pipet, the cell, and the illumination area, as well as the depth of the cell within the slice. For a given configuration, the peak amplitude of the transporter current was stable for ~30 min with repeated uncaging (Figure 4B) but became more prolonged over time (half-decay time was increased by 26.5 ± 5.9% after 30 min, $n = 4$, $p < 0.001$).

Glutamate Transporter Currents Evoked in Bergmann Glial Cells through Photolysis of MNI-D-aspartate. Astroglial cells throughout the central nervous system express glutamate transporters (*11*), but the types of transporters expressed and their density vary among cells in different brain regions. Bergmann glial cells contribute to the clearance of glutamate released at climbing fiber and parallel fiber terminals in the molecular layer of the cerebellum (*33*−*36*). To determine if MNI-D-aspartate can also be used to activate glutamate transporters in Bergmann glial cells, we made whole cell recordings from these cells in acute cerebellar slices and measured their response to uncaging of MNI-D-aspartate. As shown in Figure 5A, an inward current was triggered in Bergmann glial cells by the same uncaging conditions that were used to elicit glutamate transporter currents in astrocytes (125 μM MNI-D-aspartate, 1 ms UV exposure), and this current was similarly inhibited by TBOA (200 μM). Responses elicited from Bergmann glial cells were smaller on average than responses recorded from astrocytes (Bergmann glia, 63.2 ± 7.3 pA, $n = 7$; astrocytes, 454.5 ± 84.9 pA, $n = 4$, $p < 0.01$) and were inhibited less by TBOA (% inhibition: Bergmann glia, 81.5 ± 1.1%, $n = 7$, $p < 0.01$) (Figure 5B). These data are consistent with the lower affinity of TBOA for GLAST (*29*), the primary glutamate transporter expressed by Bergmann glia (*35*, *36*), than GLT-1, the primary glutamate transporter expressed by astrocytes (*27*). Bergmann glial responses also exhibited slower rise and decay kinetics than transporter currents recorded from astrocytes, perhaps reflecting both the lower affinity of GLAST for D-aspartate (*17*) and the lower density of transporters expressed by Bergmann glial cells (*27*).

Glutamate Transporter Currents Evoked in Purkinje Cells through Photolysis of MNI-D-aspartate. The previous results indicate that MNI-D-aspartate can be used to probe transporter activity in astroglial cells. To determine whether this compound is also suitable for monitoring glutamate transporter activity in neurons, we examined photolysis-induced responses in cerebellar Purkinje neurons. Purkinje neurons express EAAT4, a glutamate transporter that exhibits a 10-fold higher affinity for glutamate, cycles 5−10 times more

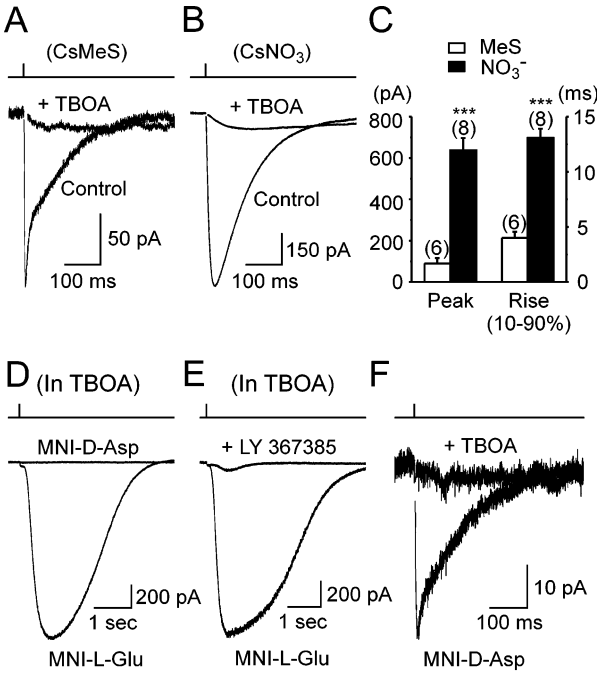

FIGURE 6: Glutamate transporter currents evoked in Purkinje neurons through photolysis of MNI-D-aspartate. (A) Inward currents recorded from a Purkinje neuron to photolysis of MNI-D-aspartate (500 μM), in the absence and presence of TBOA (200 μM). CsMeS-based internal solution. (B) Same experiment as in part A, except that the recording was made with a $CsNO_3$-based internal solution. (C) Grouped data showing the peak amplitude and 10−90% rise time of glutamate transporter currents recorded in Purkinje neurons using two different internal solutions. Numbers in parentheses indicate the number of experiments. ***$p < 0.001$. (D) Comparison of the response of a Purkinje neuron to photolysis of MNI-L-glutamate (500 μM) and MNI-D-aspartate (MNI-D-Asp, 500 μM) in the presence of TBOA (100 μM). (E) Response of a Purkinje neuron to photolysis of MNI-L-glutamate (MNI-L-Glu, 500 μM) recorded in the absence or presence of the mGluR1 selective antagonist LY 367385 (100 μM). (F) A glutamate transporter current recorded from the cell shown in part D in response to photolysis of MNI-D-aspartate. All currents were recorded at −65 mV in the presence of SR-95531 (5 μM), picrotoxin (100 μM), *R,S*-CPP (10 μM), and NBQX (15−25 μM).

slowly than other glutamate transporters, and exhibits a high permeability to anions (*37*). This transporter contributes to uptake at parallel fiber and climbing fiber synapses, and currents produced by EAAT4 cycling have been recorded in response to synaptic (*38*−*40*) and photorelease of L-glutamate (*41*, *42*) and have been used to estimate the amount of glutamate released at climbing fiber synapses (*38*−*40*). To determine if photolysis of MNI-D-aspartate is able to elicit detectible glutamate transporter currents in Purkinje neurons, we measured the response of these neurons to photolysis of 500 μM MNI-D-aspartate in the presence of ionotropic glutamate and $GABA_A$ receptor antagonists and TTX (see Materials and Methods). When the UV illumination (∼100 μm diameter spot) was centered in the molecular layer over Purkinje cell dendrites, an inward current of −89.6 ± 25.9 pA (range −41.1 to −172.6 pA, $n = 6$) was elicited following a 1 ms exposure to UV light (Figure 6A). These currents exhibited a rise time of 4.0 ± 0.6 ms and a half-decay time of 54.8 ± 3.8 ms ($n = 6$; CsMeS-based internal solution), and were inhibited by 86.3 ± 0.13% ($n = 3$) by 200 μM TBOA. These transporter currents were much smaller than the currents recorded from astrocytes or Bergmann glia under comparable conditions (see Figures 2 and 5), consistent with the lower density of transporters in Purkinje neurons (*43*). Charge movements associated with glutamate transport are enhanced in the presence of anions such as nitrate (NO_3^-) and thiocyanate (SCN^-), which permeate these transporters in a manner uncoupled from the flux of glutamate (*14*). Photolysis-induced transporter currents recorded from Purkinje neurons recorded with a $CsNO_3$-based internal solution were larger ($CsNO_3^-$: −634.4 ± 62.5 pA, $p < 0.001$) and exhibited slower rise times ($CsNO_3^-$: 13.1 ± 0.8 ms, $n = 8$, $p < 0.001$) than responses recorded with a CsMeS-based internal solution (Figure 6B,C), consistent with previous observations (*39*, *40*).

Purkinje neurons also express mGluR1, a metabotropic glutamate receptor that triggers release of calcium from internal stores and opens nonselective cation channels in the plasma membrane (*42*, *44*). Photorelease of L-glutamate has been shown to elicit inward currents mediated by mGluRs in these neurons (*42*). To determine whether the D-aspartate liberated by photolysis activates mGluRs, we compared the response of Purkinje neurons to photolysis of MNI-D-aspartate (500 μM) and MNI-L-glutamate (500 μM). In the presence of TBOA (and antagonists of AMPA, NMDA, and $GABA_A$ receptors and also TTX), photolysis of MNI-L-glutamate produced a large (−500 to −1600 pA), slowly activating, inward current in Purkinje neurons (Figure 6D) that was inhibited by 93.5 ± 2.4% ($n = 3$) by the mGluR1 antagonist LY 367385 (100 μM) (Figure 6E). This slow, inward current was not observed in response to photolysis of MNI-D-aspartate ($n = 7/7$ cells) (Figure 6D,F), even when uptake was blocked with TBOA, indicating that the released D-aspartate does not activate mGluR1. Notably, a small (∼10 pA), rapidly activating, inward current was observed in response to photolysis of MNI-L-glutamate (in the presence of 25 μM NBQX and TBOA), but not MNI-D-aspartate (see Figure 6D,E), presumably due to the activation of kainate receptors (*40*).

NMDA Receptor Activation following Photolysis of MNI-D-aspartate. Ionotropic glutamate receptors exhibit striking differences in affinity and stereoselectivity for aspartate; NMDA receptors have a similar affinity for D- and L-aspartate (D-aspartate, 10 μM; L-aspartate, 11 μM) (*18*), while AMPA receptors have an extremely low affinity for both L- and D-aspartate (*45*). To determine if MNI-D-aspartate can also be used to selectively activate NMDA receptors in neurons, we measured the response of CA1 pyramidal neurons to photolysis of MNI-D-aspartate. In the absence of antagonists of glutamate receptors or transporters, photolysis of MNI-D-aspartate produced an inward current when pyramidal neurons were held at −30 mV (Figure 7A). The current-to-voltage relationship of this response reversed at 0 mV and contained an area of negative slope conductance, characteristic of responses mediated by NMDA receptors (Figure 7B). These currents were blocked by *R,S*-CPP (10 μM) and MK-801 (50 μM), indicating that the D-aspartate released by photolysis of MNI-D-aspartate results in selective activation of NMDA receptors in CA1 pyramidal neurons (Figure 7B). Transporter currents were not observed in these neurons, presumably due to the low level of expression of EAAC1 (*11*, *32*). MNI-D-aspartate (500 μM) did not induce an outward current in neurons held at 25 mV ($n = 6$), indicating that there was little free D-aspartate in the solution and that

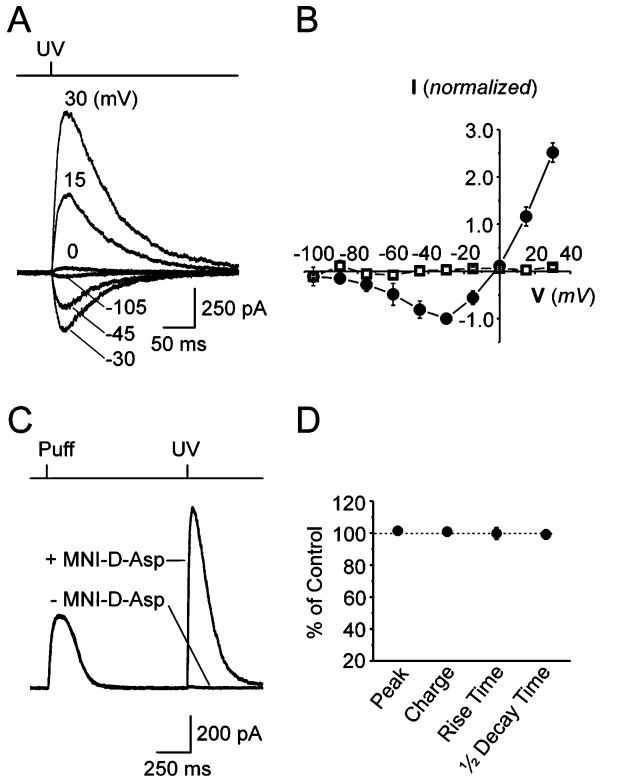

FIGURE 7: Photolysis of MNI-D-aspartate elicits NMDA receptor-mediated currents in hippocampal CA1 pyramidal neurons. (A) Response of a pyramidal neuron to photolytic release of D-aspartate recorded at different holding potentials (as indicated). The ACSF contained 1 μM TTX, and responses were recorded with a CsMeS-based internal solution. (B) Plot of the current-voltage relationship of currents recorded from CA1 pyramidal neurons in response to photolysis of MNI-D-aspartate under control conditions (closed circles) or in the presence of *R*,*S*-CPP (10 μM) and MK-801 (50 μM) (open squares). Peak amplitudes were normalized to the value recorded at $V_m = -30$ mV ($n = 3$). (C) NMDA receptor currents recorded at $V_m = 25$ mV in response to local pressure application of 500 μM D-aspartate in the presence or absence of MNI-D-aspartate (500 μM). A 1 ms UV flash was applied at the end of the recording to demonstrate the presence of the caged compound. (D) Grouped data showing the change in peak amplitude, charge transfer, 10−90% rise time, and half-decay time of transporter currents elicited through pressure application of D-aspartate, recorded in the absence and presence of 500 μM MNI-D-aspartate ($n = 6$).

MNI-D-aspartate does not activate NMDA receptors. To address whether MNI-D-aspartate acts as an inhibitor, we measured D-aspartate-evoked NMDA receptor currents in the presence or absence of MNI-D-aspartate. As shown in Figure 7C,D, MNI-D-aspartate (500 μM) did not alter the amplitude or kinetics of NMDA receptor currents evoked through focal application of D-aspartate (500 μM) ($n = 6$). These data indicate that MNI-D-aspartate is neither an agonist nor antagonist of NMDA receptors, yet it can be rapidly photolyzed by UV light to release free D-aspartate that can activate NMDA receptors in neuronal membranes.

DISCUSSION

Glutamate transporters expressed in neuronal and glial membranes set the level of ambient glutamate, shape the activation of receptors at synapses, and help maintain synapse specificity (*11*, *46*). Despite the importance of these transporters in regulating glutamate dynamics under physiological and pathological conditions, we know little about how their activity is regulated in vivo. Studies of glutamate transporters in heterologous systems have yielded conflicting results (*47*−*49*), highlighting the importance of studying these processes in their native membranes. Yet, few studies have examined the regulation of transporters in brain tissue, due to the challenges inherent in working with intact preparations. To enable such analysis, we have developed a novel caged analogue of D-aspartate (MNI-D-aspartate), because D-aspartate is efficiently transported by glutamate transporters (*17*) but has a low affinity for many glutamate receptors. We found that MNI-D-aspartate is neither an agonist nor an antagonist of glutamate transporters and is stable in aqueous solution for a period of days (in the dark at 4 °C), yet it can be photolyzed to release D-aspartate upon exposure to near-UV light. Photolysis of this compound elicited transient glutamate transporter currents in astrocytes, Bergmann glia, and Purkinje neurons in acute brain slices, but it did not activate AMPA/kainate receptors or mGluRs. Thus, the combination of MNI-D-aspartate photolysis and electrophysiological monitoring of glutamate transporter currents represents a promising approach for examining the interaction between receptors and transporters at synapses in semi-intact tissue.

Photorelease of D*-Aspartate Reveals a High Density of Transporters in Astrocyte Membranes*. Laser-induced photolysis of MNI-D-aspartate in hippocampal slices triggered an inward current in astrocytes. Because these currents were recorded in the absence of anions that exhibit a high permeability through glutamate transporters (*14*), they reflect the net influx of two positive charges that accompany each molecule of glutamate (*12*, *13*). Thus, a movement of 33.6 pC of charge (see Figure 2) corresponds to the transport of 10.5×10^7 molecules of D-aspartate and activation of an equal number of transporters, if it is assumed that the transporters complete a single cycle following brief photolysis (*16*); this assumption is based on the slow cycling time of astrocyte glutamate transporters (time constant: 35 ms) (*32*) and EAAT2 (time constant: 137 ms) (*50*) when transporting D-aspartate, as compared to the decay of the photolysis-induced transporter current (time constant: 17 ms). It is likely that this measurement underestimates the total number of transporters activated in a single cell, as some of the charge associated with transport is lost through the low resistance astrocyte membrane (*16*, *51*). It is possible that activation of glutamate transporters on a neighboring astrocyte could have contributed to the currents recorded from single astrocytes; however, previous studies suggest that the high resting conductance of the astrocyte membrane limits current spread through the astrocyte syncytium (*16*). The slow time course of these transporter currents suggests that the peak concentration of D-aspartate achieved during the 1 ms pulse was subsaturating (*30*). Together, these data indicate that a high density of functional glutamate transporters are expressed by astrocytes in this region, consistent with previous immunogold density measurements (*27*) and functional assays (*16*, *52*). By comparison, glutamate transporter currents recorded from Purkinje neurons under similar conditions (50 μm spot, 125 μM MNI-D-aspartate) were more than 100-fold smaller. To maximize the transporter current from Purkinje neurons, we increased the area of illumination and the concentration of MNI-D-aspartate. Photolyic release

of D-aspartate under these conditions resulted in the movement of ~8.4 pC of charge (see Figure 6), reflecting the activation of 2.6×10^7 transporters in these neurons, if it is assumed that only one cycle of transport is completed due to slow transport of D-aspartate by EAAT4 (*37*). Although these results indicate that there are fewer EAAT4 transporters in the membranes of Purkinje neurons (*27*, *43*), these transporters may reach a high density near synapses, particularly in perisynaptic zones that are enriched in EAAT4 (*43*). Somewhat surprisingly, glutamate transporter currents recorded from Bergmann glial cells were ~10-fold smaller than those recorded from astrocytes. This may reflect the ~2-fold lower density of glutamate transporters in Bergmann glial cell membranes (*27*) and the smaller membrane area of individual Bergmann glial cells.

Glutamate Transport Raises Extracellular K^+. In astrocyte recordings, photolysis of either MNI-D-aspartate or MNI-L-glutamate (*6*) produced a fast transient current that decayed in ~30 ms and a small tail current that decayed over several seconds. This biphasic waveform is similar to glutamate transporter currents recorded from astrocytes (*16*) and Bergmann glial cells (*34*) following electrically evoked release of glutamate from nerve terminals. It was initially proposed that the slowly decaying component of the synaptic transporter current resulted from the release of K^+ from axons following stimulation (*16*); because astrocytes exhibit a very high resting conductance to K^+, release of K^+ during axonal repolarization may shift the K^+ equilibrium potential and depolarize the astrocyte membrane. Indeed, the slow decay of the tail current is consistent with the slow clearance of K^+ from the extracellular space (*53*). Glutamate transporters counter transport one K^+ ion to complete the transport cycle (*54*), suggesting that transporter activity alone may contribute to the accumulation of K^+. In support of this conclusion, the tail current was observed following photolysis of MNI-D-aspartate when all neuronal activity was blocked. Furthermore, the amplitude of this current was the same proportion (~2%) of the peak amplitude over a wide range of light intensities, as expected if the tail current occurs as a consequence of transporter activity. The tail current depolarized astrocytes by ~1 mV in response to intense UV illumination (500 μM MNI-D-aspartate; data not shown), suggesting that glutamate transporter activity increased the extracellular concentration of K^+ by about 100 μM, assuming that the astrocyte membrane behaves like a perfect K^+ electrode. These results suggest that glutamate transporters may contribute to the rise in extracellular K^+ during periods of intense coordinated activity. By comparison, the tail current observed in astrocytes following electrical stimulation of axons was ~10% of the peak amplitude of the transporter current (*16*), indicating that the majority of the tail current recorded under these conditions results from the release of K^+ from axons rather than by transporters.

Comparison of CNB-D-aspartate and MNI-D-aspartate. A prior study examined the kinetics of transporter-associated anion currents in EAAC1-expressing HEK293 cells following photolysis of CNB-D-aspartate (*20*), a compound that has an approximately 2-fold higher quantum yield than MNI-D-aspartate (MNI-D-aspartate, 0.09; α-CNB-D-aspartate, 0.19). In these cells, D-aspartate-induced transporter currents exhibited a slower rise time than currents evoked by photolysis of CNB-L-glutamate and lacked discrete peak and steady-state components (*20*). In contrast, astrocyte transporter currents induced by photolysis of MNI-D-aspartate exhibited rise and decay kinetics that were comparable to responses evoked by MNI-L-glutamate (see Figure 2B). These results are consistent with the similar kinetics of GLT-1 transporter currents induced by L-glutamate and D-aspartate (*30*). Notably, EAAT2 (GLT-1) exhibits a higher affinity for D-aspartate than for L-glutamate (K_m: D-aspartate, 13 μM; L-glutamate, 18 μM), while EAAT3 (EAAC1) exhibits a lower affinity for D-aspartate (K_m: D-aspartate, 47 μM; L-glutamate, 28 μM)(*17*). As suggested by Grewer et al. (*20*), the slower kinetics of EAAC1 currents in response to D-aspartate may indicate that binding of D-aspartate was rate-limiting in their experiments. However, their study examined transporter-associated anion currents, which do not always mimic the movement of coupled charges (*30*). In addition, the duration of the responses triggered by CNB-D-aspartate (>120 ms) and the distinct steady-state component of the EAAC1 transporter current indicate that transporters were exposed to D-aspartate for a longer time in their experiments, which may accentuate kinetic differences among substrates. Carboxylic acids caged by esterification with the CNB chromophore have been shown to undergo (spontaneous) hydrolysis in physiological buffers (*20*, *21*). In contrast, we were unable to detect free D-aspartate in solutions of MNI-D-aspartate, indicating that this compound may be more suitable for analysis of high-affinity receptors and transporters in situ.

D-Aspartate Accumulation and Operation of Transporters in Exchange Mode. Although the rise times of astrocyte transporter currents to photorelease of D-aspartate and L-glutamate were similar, the decay of responses to D-aspartate was slightly slower (see Figure 2B). Furthermore, the decay time of D-aspartate-induced transporter currents became longer over time with repeated stimulation, an effect that was less apparent when L-glutamate was photoreleased. Transporters can, under certain conditions, operate in an exchange mode during which the movement of substrate into the cell is followed by the movement of this or another substrate back out (*54*, *55*). Such activity can prolong transporter currents and slow the clearance of substrate (*56*) and may contribute to the relatively low efficiency of glutamate transporters (*15*, *30*, *50*). Because D-aspartate is not metabolized, it is possible that the prolongation of the transporter currents results from accumulation and subsequent release of D-aspartate by homoexchange.

Cerebellar Purkinje neurons are the only neurons in the brain where glutamate transporter currents have been resolved. These neurons express EAAT4, a glutamate transporter that exhibits a high conductance to anions (*37*). Transporter currents mediated by EAAT4 have been recorded from Purkinje neurons in response to synaptic stimulation (*38*−*40*) and photorelease of glutamate (*41*, *42*). Photorelease of L-glutamate elicits a complex response resulting from the activation of AMPA, kainate, and mGluRs, in addition to glutamate transporters (*42*); in contrast, we found that photolysis of MNI-D-aspartate reliably evoked a small inward current in these neurons that was selectively mediated by glutamate transporters, as this D-aspartate-induced current was larger when recorded with a NO_3^--based internal solution and was blocked by TBOA. Purkinje cell transporter currents decayed in two phases, an initial rapid decay (to

27.2 ± 1.2% of peak in 16.8 ± 1.6 ms, $n = 6$) and a slower phase that became prominent at higher laser intensities, similar to responses observed in Purkinje neurons with 7-nitroindolinyl (NI)-caged L-glutamate when glutamate receptors were blocked (*42*). The slower phase of decay was also enhanced when Cs^+ rather than K^+ was used as the primary internal cation (data not shown). Because internal Cs^+ does not support transporter cycling as well as K^+ (*30*, *57*), internal solutions with this cation may allow a greater fraction of the transporters to operate in exchange mode (*54*). Thus, although internal Cs^+ and TEA will increase membrane resistance and improve voltage-clamp in whole-cell recordings, they may significantly disrupt transporter cycling and alter baseline synaptic currents.

MNI-D-aspartate as a Tool for Activating NMDA Receptors in Brain Slices. Unlike AMPA receptors, NMDA receptors exhibit little stereoselectivity for aspartate isomers and exhibit an affinity for aspartate that is comparable to that of L-glutamate (*18*). We found that photolysis of MNI-D-aspartate triggered NMDA receptor-mediated currents, but not AMPA-, kainate-, or mGluR-mediated currents, in hippocampal CA1 pyramidal neurons. These currents were comparable in both kinetics and amplitude to NMDA-receptor-mediated currents evoked through release of glutamate at Schaffer collateral-commissural synapses (*4*, *9*). MNI-D-aspartate did not act as an antagonist of NMDA receptors and was stable in physiological saline. A photolabile analogue of NMDA (β-DNB NMDA) has been developed as a tool for investigating the kinetics of NMDA receptors (*58*). However, because NMDA is not a substrate for glutamate transporters, clearance of NMDA within the slice is dependent on diffusion alone. As a result, photorelease of NMDA is likely to produce long-duration NMDA receptor-mediated currents, limiting temporal resolution and causing substantial receptor desensitization. The properties of MNI-D-aspartate described here suggest that it may be more suitable than caged analogues of NMDA for examining NMDA receptor function in brain slices.

REFERENCES

1. Tanaka, K., Watase, K., Manabe, T., Yamada, K., Watanabe, M., Takahashi, K., Iwama, H., Nishikawa, T., Ichihara, N., Hori, S., Takimoto, M., and Wada, K. (1997) Epilepsy and exacerbation of brain injury in mice lacking the glutamate transporter GLT-1, *Science 276*, 1699−1702.
2. Rothstein, J. D., Dykes-Hoberg, M., Pardo, C. A., Bristol, L. A., Jin, L., Kuncl, R. W., Kanai, Y., Hediger, M. A., Wang, Y., Schielke, J. P., and Welty, D. F. (1996) Knockout of glutamate transporters reveals a major role for astroglial transport in excitotoxicity and clearance of glutamate, *Neuron 16*, 675−86.
3. Carter, A. G., and Regehr, W. G. (2000) Prolonged synaptic currents and glutamate spillover at the parallel fiber to stellate cell synapse, *J. Neurosci. 20*, 4423−34.
4. Arnth-Jensen, N., Jabaudon, D., and Scanziani, M. (2002) Cooperation between independent hippocampal synapses is controlled by glutamate uptake, *Nat. Neurosci. 5*, 325−31.
5. Brasnjo, G., and Otis, T. S. (2001) Neuronal glutamate transporters control activation of postsynaptic metabotropic glutamate receptors and influence cerebellar long-term depression, *Neuron 31*, 607−16.
6. Huang, Y. H., Sinha, S. R., Tanaka, K., Rothstein, J. D., and Bergles, D. E. (2004) Astrocyte glutamate transporters regulate metabotropic glutamate receptor-mediated excitation of hippocampal interneurons, *J. Neurosci. 24*, 4551−9.
7. Clark, B. A., and Cull-Candy, S. G. (2002) Activity-dependent recruitment of extrasynaptic NMDA receptor activation at an AMPA receptor-only synapse, *J. Neurosci. 22*, 4428−36.
8. Oliet, S. H. R., Piet, R., and Poulain, D. A. (2001) Control of Glutamate Clearance and Synaptic Efficacy by Glial Coverage of Neurons, *Science 292*, 923−926.
9. Diamond, J. S. (2001) Neuronal glutamate transporters limit activation of NMDA receptors by neurotransmitter spillover on CA1 pyramidal cells, *J. Neurosci. 21*, 8328−38.
10. Asztely, F., Erdemli, G., and Kullmann, D. M. (1997) Extrasynaptic glutamate spillover in the hippocampus: Dependence on temperature and the role of active glutamate uptake, *Neuron 18*, 281−93.
11. Danbolt, N. C. (2001) Glutamate uptake, *Prog. Neurobiol. 65*, 1−105.
12. Zerangue, N., and Kavanaugh, M. P. (1996) Flux coupling in a neuronal glutamate transporter, *Nature 383*, 634−7.
13. Levy, L. M., Warr, O., and Attwell, D. (1998) Stoichiometry of the glial glutamate transporter GLT-1 expressed inducibly in a Chinese hamster ovary cell line selected for low endogenous Na+-dependent glutamate uptake, *J. Neurosci. 18*, 9620−8.
14. Wadiche, J. I., Amara, S. G., and Kavanaugh, M. P. (1995) Ion fluxes associated with excitatory amino acid transport, *Neuron 15*, 721−8.
15. Otis, T. S., and Jahr, C. E. (1998) Anion currents and predicted glutamate flux through a neuronal glutamate transporter, *J. Neurosci. 18*, 7099−110.
16. Bergles, D. E., and Jahr, C. E. (1997) Synaptic activation of glutamate transporters in hippocampal astrocytes, *Neuron 19*, 1297−308.
17. Arriza, J. L., Fairman, W. A., Wadiche, J. I., Murdoch, G. H., Kavanaugh, M. P., and Amara, S. G. (1994) Functional comparisons of three glutamate transporter subtypes cloned from human motor cortex, *J. Neurosci. 14*, 5559−69.
18. Olverman, H. J., Jones, A. W., Mewett, K. N., and Watkins, J. C. (1988) Structure/activity relations of *N*-methyl-D-aspartate receptor ligands as studied by their inhibition of [^{3}H]D-2-amino-5-phosphonopentanoic acid binding in rat brain membranes, *Neuroscience 26*, 17−31.
19. Canepari, M., Nelson, L., Papageorgiou, G., Corrie, J. E., and Ogden, D. (2001) Photochemical and pharmacological evaluation of 7-nitroindolinyl-and 4-methoxy-7-nitroindolinyl-amino acids as novel, fast caged neurotransmitters, *J. Neurosci. Methods 112*, 29−42.
20. Grewer, C., Madani Mobarekeh, S. A., Watzke, N., Rauen, T., and Schaper, K. (2001) Substrate translocation kinetics of excitatory amino acid carrier 1 probed with laser-pulse photolysis of a new photolabile precursor of D-aspartic acid, *Biochemistry 40*, 232−40.
21. Pettit, D. L., Wang, S. S., Gee, K. R., and Augustine, G. J. (1997) Chemical two-photon uncaging: A novel approach to mapping glutamate receptors, *Neuron 19*, 465−71.
22. Amit, B., Ben-Efraim, D. A., and Patchornik, A. (1976) LIght-sensitive amides. The photosolvolysis of substituted 1-acyl-7-nitroindolines, *J. Am. Chem. Soc. 98*, 843−844.
23. Li, X., Atkinson, R., and King, S. (2001) Preparation and evaluation of new -canavanine derivatives as nitric oxide synthase inhibitors, *Tetrahedron 57*, 6557−6565.
24. Matsuzaki, M., Ellis-Davies, G. C., Nemoto, T., Miyashita, Y., Iino, M., and Kasai, H. (2001) Dendritic spine geometry is critical for AMPA receptor expression in hippocampal CA1 pyramidal neurons, *Nat. Neurosci. 4*, 1086−92.
25. Ellis-Davies, G. C., and Kaplan, J. H. (1994) Nitrophenyl-EGTA, a photolabile chelator that selectively binds Ca2+ with high affinity and releases it rapidly upon photolysis, *Proc. Natl. Acad. Sci. U.S.A. 91*, 187−91.
26. Norman, R. O., and Radda, G. K. (1961) *J. Chem. Soc.* 3030−3036.
27. Lehre, K. P., and Danbolt, N. C. (1998) The number of glutamate transporter subtype molecules at glutamatergic synapses: Chemical and stereological quantification in young adult rat brain, *J. Neurosci. 18*, 8751−7.
28. Shigeri, Y., Shimamoto, K., Yasuda-Kamatani, Y., Seal, R. P., Yumoto, N., Nakajima, T., and Amara, S. G. (2001) Effects of threo-beta-hydroxyaspartate derivatives on excitatory amino acid transporters (EAAT4 and EAAT5), *J. Neurochem. 79*, 297−302.
29. Shimamoto, K., Lebrun, B., Yasuda-Kamatani, Y., Sakaitani, M., Shigeri, Y., Yumoto, N., and Nakajima, T. (1998) DL-threo-beta-benzyloxyaspartate, a potent blocker of excitatory amino acid transporters, *Mol. Pharmacol. 53*, 195−201.

30. Bergles, D. E., Tzingounis, A. V., and Jahr, C. E. (2002) Comparison of coupled and uncoupled currents during glutamate uptake by GLT-1 transporters, *J. Neurosci. 22*, 10153−62.
31. Wadiche, J. I., Arriza, J. L., Amara, S. G., and Kavanaugh, M. P. (1995) Kinetics of a human glutamate transporter, *Neuron 14*, 1019−27.
32. Bergles, D. E., and Jahr, C. E. (1998) Glial contribution to glutamate uptake at Schaffer collateral-commissural synapses in the hippocampus, *J. Neurosci. 18*, 7709−16.
33. Bergles, D. E., Dzubay, J. A., and Jahr, C. E. (1997) Glutamate transporter currents in bergmann glial cells follow the time course of extrasynaptic glutamate, *Proc. Natl. Acad. Sci. U.S.A. 94*, 14821−5.
34. Clark, B. A., and Barbour, B. (1997) Currents evoked in Bergmann glial cells by parallel fibre stimulation in rat cerebellar slices, *J. Physiol. (London) 502*, 335−50.
35. Rothstein, J. D., Martin, L., Levey, A. I., Dykes-Hoberg, M., Jin, L., Wu, D., Nash, N., and Kuncl, R. W. (1994) Localization of neuronal and glial glutamate transporters, *Neuron 13*, 713−25.
36. Lehre, K. P., Levy, L. M., Ottersen, O. P., Storm-Mathisen, J., and Danbolt, N. C. (1995) Differential expression of two glial glutamate transporters in the rat brain: Quantitative and immunocytochemical observations, *J. Neurosci. 15*, 1835−53.
37. Fairman, W. A., Vandenberg, R. J., Arriza, J. L., Kavanaugh, M. P., and Amara, S. G. (1995) An excitatory amino acid transporter with properties of a ligand-gated chloride channel, *Nature 375*, 599−603.
38. Otis, T. S., Kavanaugh, M. P., and Jahr, C. E. (1997) Postsynaptic glutamate transport at the climbing fiber-Purkinje cell synapse, *Science 277*, 1515−8.
39. Auger, C., and Attwell, D. (2000) Fast removal of synaptic glutamate by postsynaptic transporters, *Neuron 28*, 547−58.
40. Huang, Y. H., Dykes-Hoberg, M., Tanaka, K., Rothstein, J. D., and Bergles, D. E. (2004) Climbing fiber activation of EAAT4 transporters and kainate receptors in cerebellar Purkinje cells, *J. Neurosci. 24*, 103−11.
41. Brasnjo, G., and Otis, T. S. (2004) Isolation of glutamate transport-coupled charge flux and estimation of glutamate uptake at the climbing fiber-Purkinje cell synapse, *Proc. Natl. Acad. Sci. U.S.A. 101*, 6273−6278.
42. Canepari, M., Papageorgiou, G., Corrie, J. E., Watkins, C., and Ogden, D. (2001) The conductance underlying the parallel fibre slow EPSP in rat cerebellar Purkinje neurones studied with photolytic release of L-glutamate, *J. Physiol. 533*, 765−72.
43. Dehnes, Y., Chaudhry, F. A., Ullensvang, K., Lehre, K. P., Storm-Mathisen, J., and Danbolt, N. C. (1998) The glutamate transporter EAAT4 in rat cerebellar Purkinje cells: A glutamate-gated chloride channel concentrated near the synapse in parts of the dendritic membrane facing astroglia, *J. Neurosci. 18*, 3606−19.
44. Kim, S. J., Kim, Y. S., Yuan, J. P., Petralia, R. S., Worley, P. F., and Linden, D. J. (2003) Activation of the TRPC1 cation channel by metabotropic glutamate receptor mGluR1, *Nature 426*, 285−91.
45. Patneau, D. K., and Mayer, M. L. (1990) Structure−activity relationships for amino acid transmitter candidates acting at *N*-methyl-D-aspartate and quisqualate receptors, *J. Neurosci. 10*, 2385−99.
46. Huang, Y. H., and Bergles, D. E. (2004) Glutamate transporters bring competition to the synapse, *Curr. Opin. Neurobiol. 14*, 346−52.
47. Dowd, L. A., and Robinson, M. B. (1996) Rapid stimulation of EAAC1-mediated Na^+-dependent L-glutamate transport activity in C6 glioma cells by phorbol ester, *J. Neurochem. 67*, 508−16.
48. Trotti, D., Peng, J. B., Dunlop, J., and Hediger, M. A. (2001) Inhibition of the glutamate transporter EAAC1 expressed in Xenopus oocytes by phorbol esters, *Brain Res. 914*, 196−203.
49. Gonzalez, M. I., and Robinson, M. B. (2004) Neurotransmitter transporters: Why dance with so many partners? *Curr. Opin. Pharmacol. 4*, 30−5.
50. Wadiche, J. I., and Kavanaugh, M. P. (1998) Macroscopic and microscopic properties of a cloned glutamate transporter/chloride channel, *J. Neurosci. 18*, 7650−61.
51. Dzubay, J. A., and Jahr, C. E. (1999) The concentration of synaptically released glutamate outside of the climbing fiber-Purkinje cell synaptic cleft, *J. Neurosci. 19*, 5265−74.
52. Diamond, J. S., and Jahr, C. E. (2000) Synaptically released glutamate does not overwhelm transporters on hippocampal astrocytes during high-frequency stimulation, *J. Neurophysiol. 83*, 2835−43.
53. Aitken, P. G., and Somjen, G. G. (1986) The sources of extracellular potassium accumulation in the CA1 region of hippocampal slices, *Brain Res. 369*, 163−7.
54. Kanner, B. I., and Bendahan, A. (1982) Binding order of substrates to the sodium and potassium ion coupled L-glutamic acid transporter from rat brain, *Biochemistry 21*, 6327−30.
55. Dunlop, J. (2001) Substrate exchange properties of the high-affinity glutamate transporter EAAT2, *J. Neurosci. Res. 66*, 482−6.
56. Isaacson, J. S., and Nicoll, R. A. (1993) The uptake inhibitor L-trans-PDC enhances responses to glutamate but fails to alter the kinetics of excitatory synaptic currents in the hippocampus, *J. Neurophysiol. 70*, 2187−91.
57. Barbour, B., Brew, H., and Attwell, D. (1991) Electrogenic uptake of glutamate and aspartate into glial cells isolated from the salamander (Ambystoma) retina, *J. Physiol. (London) 436*, 169−93.
58. Gee, K. R., Niu, L., Schaper, K., Jayaraman, V., and Hess, G. P. (1999) Synthesis and photochemistry of a photolabile precursor of *N*-methyl-D-aspartate (NMDA) that is photolyzed in the microsecond time region and is suitable for chemical kinetic investigations of the NMDA receptor, *Biochemistry 38*, 3140−7.

BI048051M